



Universiteit
Leiden
The Netherlands

Inducing spin triplet superconductivity in a ferromagnet

Voltan, S.

Citation

Voltan, S. (2016, September 29). *Inducing spin triplet superconductivity in a ferromagnet. Casimir PhD Series*. Retrieved from <https://hdl.handle.net/1887/43299>

Version: Not Applicable (or Unknown)

License:

Downloaded from: <https://hdl.handle.net/1887/43299>

Note: To cite this publication please use the final published version (if applicable).

Cover Page



Universiteit Leiden



The handle <http://hdl.handle.net/1887/43299> holds various files of this Leiden University dissertation

Author: Voltan, Stefano

Title: Inducing spin triplet superconductivity in a ferromagnet

Issue Date: 2016-09-29

6

PERPENDICULAR UPPER CRITICAL FIELD IN A TRIPLET SPIN VALVE

A superconducting triplet spin valve (TSV) based on the half-metallic CrO₂ can show “colossal” variations of the critical temperature, up to more than 1 K. Here we investigate further such TSV devices looking at the dependence of the perpendicular upper critical field $H_{c2\perp}$ on the temperature. What we observe is an interesting and peculiar behavior: there is a clear deviation from the universal linear dependence and the average slope is suppressed much more than what can be described with the formalism used for conventional proximized structures.

Contents

6.1	Introduction	107
6.2	Experimental details	108
6.3	Perpendicular upper critical field $H_{c2\perp}$	108
6.3.1	$H_{c2\perp}$ of the S layer and of S/F hybrids	108
6.3.2	$H_{c2\perp}$ of triplet spin valve structures	114
6.4	Conclusions	116

Parts of this chapter have been published in:

S. Voltan, A. Singh, and J. Aarts. Triplet generation and upper critical field in superconducting spin valves based on CrO₂, *Phys. Rev. B* **94**, 054503 (2016).

6.1 Introduction

In Chap.5, by using TSVs based on the half-metallic CrO_2 we could show a huge T_c suppression, well over 1 K. Such a large effect is more than an order of magnitude bigger than for TSVs based on standard ferromagnets [1–3]. An explanation for this was recently given by Mironov and Buzdin [5], who showed that the special boundary conditions for a S/F/HM system (as opposed to an S/ F_1 / F_2 system) lead to the appearance of an extra triplet component in the S and F layers, with a much stronger effect on T_c of the spin valve as a consequence. In the experiments presented in Chap.5, to induce the magnetic non-collinearity between F_1 and F_2 , the magnetic field was rotated from in-plane to out-of-plane. For this reason we had to ascertain that the measured δT_c was not due to the difference between the parallel and perpendicular upper critical field H_{c2} . In particular, in the out-of-plane configuration, several spurious effects such as vortices and stray field of the magnetic layers can influence the superconducting properties. This problem was circumvented by comparing the behavior of the TSV to equivalent structures where either the F_1 or the F_2 layer was removed, so where the triplet generation was not expected. However, measuring H_{c2} as function of temperature would actually provide a more fundamental description of the TSV effect. The study of H_{c2} not only quantifies the efficiency of triplet generation but also probes the change in behavior of the superconductor due to the triplet proximity effect.

Here we study S/ F_1 / N / F_2 TSVs based on CrO_2 (F_2 layer), similar to the ones studied in Chap.5, with MoGe as S layer and Ni as mixer layer (F_1), looking at a different aspect, which has not been explored so far. We address the effect of the triplet generation on the phase diagram of the superconductor $H_{c2\perp}(T)$. For the reasons explained above, $H_{c2\perp}(T)$ of the stack seems to be a more fundamental quantity to study the TSVs, particularly in our device geometry. With the field applied out-of-plane (the TSV is “on”) we observe an unexpected behavior: the $H_{c2\perp}(T)$ phase diagram strongly deviates from the universal linear behavior observed for both isolated superconductors and structures with no triplet generation. Next to that, there is a strong suppression of the critical field, namely a decrease of the average slope, which cannot be described with the standard formalism for proximized S/F hybrids. The link between triplet generation and $H_{c2\perp}(T)$ dependence is confirmed by comparing TSVs with different Ni thickness, so with different efficiency in triplet generation. We show how this reflects in a very different critical field behavior, the study of which can be used to have insightful information about the triplet generation.

In Sec.6.2 we describe sample preparation and measurement details while in Sec.6.3

we show the results for the temperature dependence of the perpendicular upper critical field for the TSVs (Sec.6.3.2) compared with the isolated superconductor and the S/F hybrids in absence of triplet generation (Sec.6.3.1). To conclude, in Sec.6.4 we highlight the main results of our study.

6.2 Experimental details

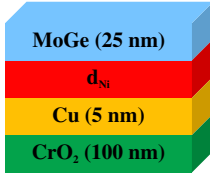


Figure 6.1: Sketch which shows the four layers forming the TSV, with their respective thickness. d_{Ni} was varied, with values $d_{\text{Ni}} = 0, 1.0, 1.5, 2.2$ and 3.0 nm.

Our TSV device is a stack of four layers namely MoGe(25)/Ni(d_{Ni})/Cu(5)/CrO₂(100) (see Fig.6.1a), where the numbers express the thickness in nanometers. The thickness of the mixer layer was varied, with values $d_{\text{Ni}} = 0, 1.0, 1.5, 2.2$ and 3.0 nm. The devices studied here are the same presented in Sec.5.3.3, where we looked at the dependence of the TSV effect (measured by the T_c variation) on d_{Ni} . Therefore, the preparation procedure as well as the device geometry are identical as in Chap.5 and they have been de-

scribed in Sec.5.2. A micrograph of the device is shown in Fig.5.1b. As in Chap.5 we performed electrical measurements in a physical properties measurement system and the angle θ between the surface plane and the applied magnetic field H_a (see Fig.5.3a), in this case was fixed to $\theta = 90$. Thus, the $R(H)$ measurements (Sec.6.3) were only performed in the out-of-plane configuration.

6.3 Perpendicular upper critical field $H_{c2\perp}$

6.3.1 $H_{c2\perp}$ of the S layer and of S/F hybrids

We first characterize our system in absence of triplet generation. We measured the resistance vs magnetic field dependence $R(H_a)$ at different temperatures for: i) a MoGe(25) single film, to characterize the isolated superconductor, ii) a trilayer MoGe(25)/Ni(1.5)/Cu(5), and iii) a trilayer MoGe(25)/Cu(5)/CrO₂(100) (Fig.6.2a, b, and c respectively). Cases ii) and iii) are studied to look at the pair-breaking effect due to either the Ni or the CrO₂ layer, independently. The Cu layer, used in the TSV only to decouple the ferromagnets, is much thinner than the coherence length ξ_N (of

the order of $1 \mu\text{m}$) so it does not play a role in suppressing the order parameter. For all the measurements presented in this section the field was applied perpendicular to the plane of the structure, in order to have a reference for the TSV effect, which is maximized when the field is applied in this geometry.

In Fig.6.2 we can immediately notice a large difference in the normal resistance R_N of the three structures: 840Ω for the isolated MoGe (Fig.6.2a), 240Ω for the trilayer MoGe/Ni/Cu (Fig.6.2b) and 4.5Ω for the trilayer MoGe/Cu/CrO₂ (Fig.6.2c). Above T_c , the MoGe has high resistivity ($\rho_{\text{MoGe}} = 200 \mu\Omega\text{cm}$) and therefore is shorted by the Cu layer ($\rho_{\text{Cu}} = 2 \mu\Omega\text{cm}$) in ii) and by CrO₂ ($\rho_{\text{CrO}_2} = 2 \mu\Omega\text{cm}$) in iii). The low value of R_N for MoGe/Cu/CrO₂ is due to the fact that the CrO₂ is not patterned. In addition it is an indication of a good interface transparency, as explained in Chap.5. The peak at the onset of the superconductivity, observed for $R(T)$ curves and discussed in Sec.5.3.2, is clearly visible also for the $R(H)$ curves of the trilayer MoGe/Cu/CrO₂. The peak becomes broader when lowering the temperature.

For the isolated MoGe and the trilayer MoGe/Ni/Cu the value of $H_{c2\perp}$ is extrapolated as shown by the black dashed lines in Fig.6.2a, as the field value at which the fitting line of the linear part of the transition intersects the R_N value. This is a standard construction for cases when the S-layer is weakly pinning and freely flowing vortices lead to a flux flow resistance $\rho_f = H/H_{c2} \cdot \rho_N$ [6].

For the trilayer MoGe/Cu/CrO₂ (see Fig.6.2c), the shape of the transition is very different because of the feature described in Sec.5.3.2. In addition it is important to point out that the total resistance we measure is the result of the parallel between MoGe which is highly resistive and the other layers. The contribution to the resistance due to vortex motion is $R_f = H/H_{c2} \cdot R_N$. In the normal state, the resistance of the superconducting layer R_N is about 840Ω and it is shorted by the low resistive CrO₂ layer ($R_{\text{CrO}_2} \approx 2 \Omega$). Therefore for the stack MoGe/Cu/CrO₂ (and the TSVs) only the lowest fraction (0.2%) of vortex resistance contributes to the total resistance in the observed transitions. In this region the flow of vortices is not coherent and the dependence of the resistance on the magnetic field is not linear. For this reason the method shown in Fig.6.2a is no longer justified to determine H_{c2} , also because too little is known about vortex dynamics in proximized systems. The only reliable way we have in this case to define $H_{c2\perp}$, is to consider the field at which, coming from the normal state, the resistance starts to increase as shown in Fig.6.2c (H_{c2_u} value). The operational threshold is 0.3 times the peak height above the normal value R_N , namely $R_N + 0.3 \cdot (R_{\text{max}} - R_N)$, where R_{max} is the maximum resistance value of the peak. As explained above, the peak originates from the breaking of Cooper pairs and start to set in at the onset of

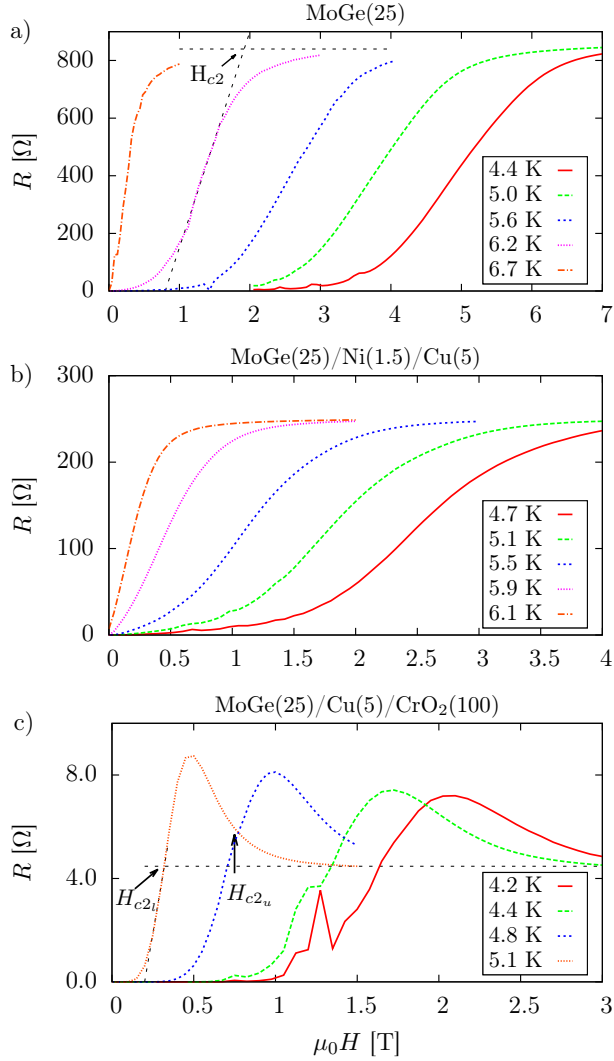


Figure 6.2: Plots of the resistance as a function of the magnetic field (applied out-of-plane) at different temperatures for: a) an isolated superconductor MoGe(25), b) a trilayer MoGe(25)/Ni(1.5)/Cu(5) and c) a trilayer MoGe(25)/Cu(5)/CrO₂(100). Dashed black lines in a) and c) show how the upper critical field $H_{c2\perp}$ has been defined: as the field value at which the fitting line of the linear part of the transition intersects the R_N value.

superconductivity, even if not necessarily of the proximity effect. Therefore this value, which we call H_{c2u} , is an upper limit for the real upper critical field, which could be a bit lower. For comparison we also look at the dependence of the field value defined as in Fig.6.2a, because only below this value the resistance drops to zero. This value, which we call H_{c2l} (see Fig.6.2c), represents a lower limit for the real $H_{c2\perp}$. Also, representing the onset of flux flow, it is definitely related to $H_{c2\perp}$.

Very small oscillations, possibly due to vortex dynamics, are visible at high fields in the tail of the transition curve for the lowest temperatures in Fig.6.2a and 6.2b. The oscillations become much more evident for the trilayer MoGe/Cu/CrO₂ (Fig.6.2c), in particular at 4.2 K and 4.4 K at around 1.2 T. Here the total resistance of the multilayer is low, so the relative contribution of the oscillations, which seems to be of the order a few ohms is more relevant. The sharpness of the oscillation at 4.2 K is an artifact due to the limited amount of points acquired for that specific measurement. For the curves where big oscillations are present we fitted the background transition, after subtracting the oscillating contributions. Since the oscillations are superimposed to the resistance curve of the superconductor, they do not contribute to the proximity effect and do not change the slope of the curve, so the value of $H_{c2\perp}$.

Fig.6.3 shows the phase diagrams $H_{c2\perp}$ vs T obtained from Figs.6.2a (circles), b (squares) and c (full and empty triangles, for H_{c2u} and H_{c2l} respectively). To quantitatively analyze proximized systems, the formalism presented by Fominov et al. in

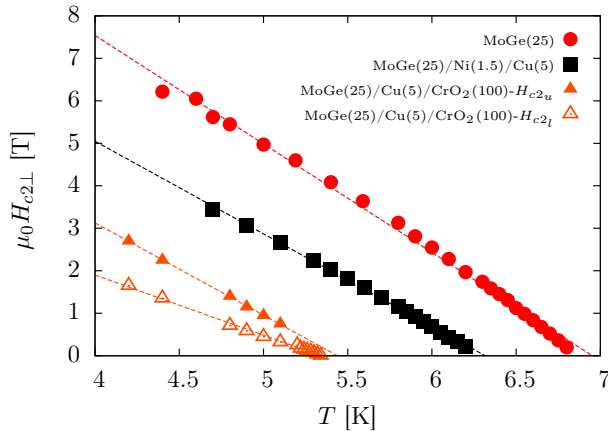


Figure 6.3: Phase diagram $H_{c2\perp}$ vs T for the devices of Fig.6.2. For MoGe(25) the dashed line results from fitting Eq.(6.1,6.2), for the other sets of data from fitting Eq.(6.4).

Ref. [7] is typically used. The formalism, based on the quasiclassical Usadel equations which describe the gap- and pair-correlation functions, was originally developed to describe proximity effects in S/N systems, in particular the behavior of T_c as function of such parameters as layer thicknesses, interface transparency, and diffusion constants. It was extended to S/F hybrids with F a weak ferromagnet in the dirty limit (the mean free ℓ path is the shortest length after the Fermi wave length), starting from the linearized Usadel equations. In many cases the so-called single-mode approximation (SMA) can be used and the final equations reduce to

$$\ln(t_0) = \Psi\left(\frac{1}{2}\right) - \Psi\left(\frac{1}{2} - \frac{\Omega^2}{2t_0}\right) \quad (6.1)$$

$$\Omega \tan\left(\Omega \frac{d_S}{\xi_S}\right) = \frac{\gamma}{\gamma_b} \quad (6.2)$$

where $t_0 = T_c/T_{cS}$ is the critical temperature of the proximized system T_c , normalized by the critical temperature of the isolated superconductor T_{cS} , d_S is the thickness of the superconductor, $\xi_S = (2/\pi)\xi_{S0}$, with ξ_{S0} the Ginzburg-Landau coherence length, Ψ the digamma function and Ω is the pair-breaking parameter responsible for the suppression of T_c . As can be seen from Eq.(6.2), Ω depends on γ , which measures the strength of the proximity effect, and on γ_b which describes the effect of the boundary transparency [8]. These equations allow to describe the T_c variation as function of the layer thickness (either of S or F), at zero field. Due to the additivity of the pair-breaking [9], it is trivial to extend the formalism to include the role of the magnetic field, as shown in Ref. [10]. In this case in Eq.(6.1,6.2) Ω^2 is substituted by

$$\Omega^2(t) = \Omega_0^2 + h_{c2\perp}(t), \quad (6.3)$$

where $t = T/T_{cS}$ and $h_{c2\perp}(t) = (2\pi/\phi_0)H_{c2\perp}\xi_S^2$. Ω_0^2 is the pair-breaking parameter at zero field. By combining Eq.(6.1, 6.2, 6.3) and solving them numerically is possible to obtain and fit the H_{c2} vs T dependence. Close to T_c (smaller critical fields), the dependence is linear.

The isolated superconductor can be described by the equations above in the limit $\Omega_0 \rightarrow 0$. The T_c of MoGe is approximately 6.9 K, close to the bulk value [11]. By fitting the curve we obtain $\xi_S \simeq 2.7$ nm which gives a coherence length $\xi_{S0} \simeq 4.2$ nm, consistent with what is reported in literature for MoGe [11]. The same result for ξ_{S0} can be obtained from Ginzburg-Landau by the linear relation which describes the perpen-

dicular H_{c2} dependence of a superconducting film near T_c :

$$\mu_0 H_{c2\perp} = \frac{\phi_0}{2\pi\xi_{S0}^2} \left(1 - \frac{T}{T_c}\right), \quad (6.4)$$

where ϕ_0 is the magnetic quantum flux.

In our trilayer MoGe/Ni/Cu, Ni is a relatively strong ferromagnet (exchange energy $E_{ex} \simeq$). This raises the question about the validity of Usadel equations (dirty limit). The two main conditions for the validity are: i) $E_{ex} \ll E_F$, with E_F the Fermi energy, and ii) $\xi_F = \sqrt{\hbar D_F / E_{ex}} \gg \ell$, with D_F the diffusion coefficient of F and ℓ the mean free path. If we take a Fermi velocity $v_F = 10^6$ m/s and we calculate D_F from v_F and the experimental resistivity $\rho_{Ni} = 7 \mu\Omega\text{cm}$, the estimated values are $E_F \simeq 2.8$ eV, $\xi_F \simeq 1.5$ nm and $\ell \simeq 5.4$ nm. While i) is satisfied, ii) is not. However the Ni layer of our system is really thin and the value of ℓ , calculated from the resistivity measured for much thicker films, could be overestimated. If we assume that the Usadel equations are valid and we try to fit the trilayer data with Eq.(6.1,6.2,6.3), we obtain $\xi_{S0} \simeq 4.5$ nm, a value close to the one of the isolated MoGe, but the T_c suppression from 7.0 K to 6.3 K cannot be reproduced. The minimum T_c we can obtain (in the case of very small γ_b) is 6.5 K, a signal that the SMA (often used in the limit of thin superconductors) cannot properly describe our data. It is possible that the multi mode method or the method of fundamental solution [7] could provide more accurate results but more likely a new formalism specifically developed for strong ferromagnets is needed. The analysis above certainly cannot be applied to the trilayer MoGe/Cu/CrO₂ where the proximity is with a thick half-metallic ferromagnet. In this case as expected T_c is suppressed even more, to a value of about 5.4 K.

Even if we cannot have quantitative information about the proximity from the analysis above, we can qualitatively see that the effect of the pair-breaking is a simple shift of the $H_{c2}(T)$ curve towards lower T_c values. The slope, dependent only on ξ_S which is an intrinsic property of the superconductor not affected by the pair-breaking, should remain unchanged. This is what we observe for the trilayer MoGe/Ni/Cu and for MoGe/Cu/CrO₂, if we consider H_{c2_u} . Instead, $H_{c2_l}(T)$ shows a lower slope. This observation seems to suggest that H_{c2_u} is the proper definition of $H_{c2\perp}$. However, since a certain amount of triplet generation cannot be completely excluded in this case (as mentioned in Sec.5.3.2), the behavior of H_{c2_u} could simply describe the dependence of the superconductor before the CrO₂ gets proximized.

6.3.2 $H_{c2\perp}$ of triplet spin valve structures

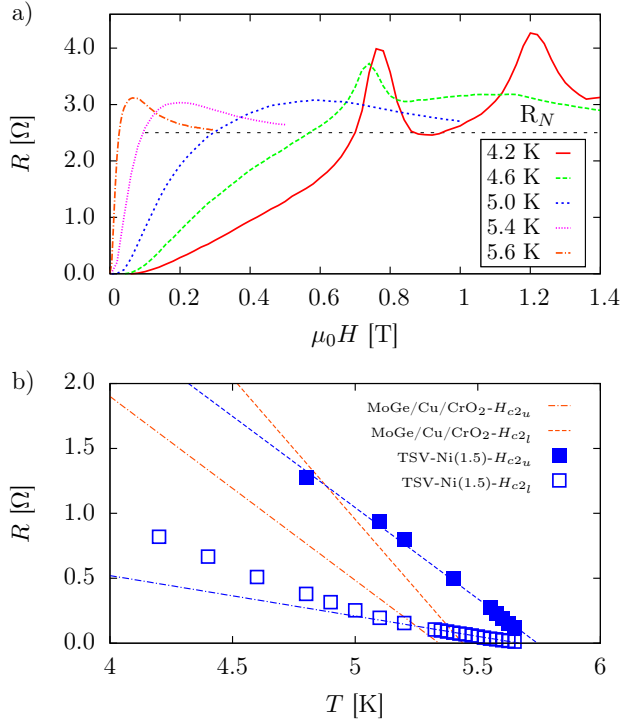


Figure 6.4: $R(H)$ curves at different temperatures (a) and phase diagram $H_{c2\perp}(T)$ (b), for the TSV MoGe(25)/Ni(1.5)/Cu(5)/CrO₂(100). b) is a zoom of the curve plotted in Fig.6.3c. The dashed line is the linear fit of the points with $T > 0.85 \cdot T_c$.

As we can see from Fig.6.4b the full TSV shows a behavior very different from the trilayers. In Fig.6.4b we show the phase diagram for the superconducting triplet spin valve MoGe(25)/Ni(1.5)/Cu(5)/CrO₂(100) compared with the trilayer MoGe(25)/Cu(5)/CrO₂(100), for both H_{c2u} (dashed lines, full squares) and H_{c2l} (dot-dash lines, empty squares), defined as described in Sec.6.3.1 (Fig.6.2c). A selection of the $R(H)$ transitions for the TSV, from which the values of H_{c2u} and H_{c2l} are obtained, is shown in Fig.6.4a. The feature observed, namely the peak at the onset of the transition and the oscillations visible at around 0.8 and 1.2 T, have been extensively discussed in Sec.5.3.2 and 6.3.1.

The critical temperature of the TSV, about 5.7 K, is slightly higher than the trilayer

MoGe/Cu/CrO₂ where there is no (or little) triplet generation. This is not consistent with what expected and with what observed in Chap.5 and it is likely due to differences between the interface transparencies of the samples we compare. If we look at H_{c2_u} the relation is linear but with a significantly lower slope, 0.65 times the slope of the trilayer. This suggests that what we observe for a TSV is not simply a pair-breaking due to S/F proximity, but a stronger effect due to the leakage of triplets in the ferromagnet. In this case the multilayer behaves more like an S/N than an S/F proximized system.

If we look at H_{c2_l} , the slope is suppressed even more. Here, we see another interesting and unexpected feature: the dependence is linear very close to T_c but at around $T = 0.85 \cdot T_c$ it strongly deviates to higher values. Interestingly enough, this unusual behavior is pronounced for TSV-Ni(1.5) and TSV-Ni(1.0) and it gradually disappears by increasing or decreasing the Ni thickness. This seems to suggest a relation between non-linearity and triplet generation. In Sec.6.3.1 we addressed the problem of large oscillations in the transition curves at low temperatures. The lower the temperature (higher critical field) the more oscillation modes included in the transition. For this reason we have to point out that the values extrapolated at lower temperatures are less precise. However the range of variation is not such to modify the qualitative behavior of our observation. Moreover at low fields no oscillations are present so that the definition of the slope of the curve is not affected by that. A similar non-linear behavior has been reported in Ref. [12] for Nb/Cu bilayers. The authors propose several, although not conclusive, explanations for the observation, but in general the effect is attributed to the proximity effect and the boundary conditions. Even if we do not have enough elements to claim that the physical mechanism for the similar behavior is the same, such effects observed in an S/N bilayer seem to be consistent with what we measure in a S/F-type structure with a long-range proximity effect.

If we compare the slope of the phase diagram for TSVs with different Ni thickness, we expect a stronger effect the closer to the optimum value we are. This is confirmed by the experimental results shown in Fig.6.5, where we plot the absolute value of the slope obtained by the fit of the $H_{c2_u}(T)$ curves as a function of the Ni thickness. Dashed and dot-dash lines show the value for the isolated MoGe(25) and the trilayer MoGe(25)/Ni(1.5)/Cu(5), respectively. As for the T_c variation (Fig.5.9), we observe a non-monotonic behavior, with a maximum effect between 1.0 and 1.5 nm. A similar value has been obtained for the δT_c dependence. This suggests that there is a direct correlation between slope of the $H_{c2_u}(T)$ curve and the TSV efficiency, namely the triplet generation.

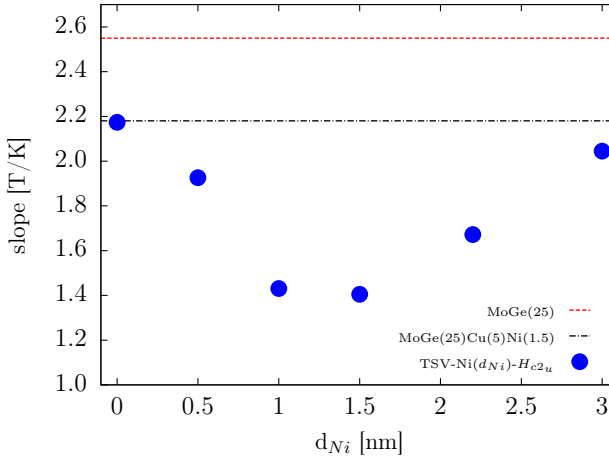


Figure 6.5: Slope of the linear fit of curve $H_{c2u}(T)$ as a function of the thickness of the Ni layer d_{Ni} (squares). Dashed to dot-dash lines show the value for the isolated MoGe(25) and the trilayer MoGe(25)/Ni(1.5)/Cu(5), respectively.

6.4 Conclusions

To summarize we studied the dependence of the perpendicular upper critical field as function of the temperature for a TSV. The determination of the actual H_{c2} value is complicated by the presence of the spin accumulation peak, however we could define an upper and lower limit, H_{c2u} and H_{c2l} , which allowed us to compare the TSVs with the systems with no triplet generation. The behavior is very different from the standard S/F proximized systems: the slope is strongly suppressed, similarly to what happens in S/N systems, and for $H_{c2l}(T)$ we observe a clear deviation from the universal linear dependence. Both effects are prominent for Ni thicknesses around 1.5 nm and vanish for thinner or thicker Ni layers, which indicates a link with the efficiency of the triplet generation. This behavior cannot be described by simple pair breaking, as described by the formalism developed so far for S/F hybrids. A new theoretical formalism along the lines of Ref. [5] is needed to describe the behavior of the critical field in presence of triplet superconductivity.

BIBLIOGRAPHY

- [1] P. V. Leksin, N. N. Garif'yanov, I. A. Garifullin, Y. V. Fominov, J. Schumann, Y. Krupskaya, V. Kataev, O. G. Schmidt, and B. Buechner. Evidence for triplet superconductivity in a superconductor-ferromagnet spin valve. *Phys. Rev. Lett.* **109**, 057005 (2012).
- [2] X. L. Wang, A. Di Bernardo, N. Banerjee, A. Wells, F. S. Bergeret, M. G. Blamire, and J. W. A. Robinson. Giant triplet proximity effect in superconducting pseudo spin valves with engineered anisotropy. *Phys. Rev. B* **89**, 140508 (2014).
- [3] M. G. Flokstra, T. C. Cunningham, J. Kim, N. Satchell, G. Burnell, P. J. Curran, S. J. Bending, C. J. Kinane, J. F. K. Cooper, S. Langridge, A. Isidori, N. Pugach, M. Eschrig, and S. L. Lee. Controlled suppression of superconductivity by the generation of polarized Cooper pairs in spin-valve structures. *Phys. Rev. B* **91**, 060501 (2015).
- [4] A. Singh, S. Voltan, K. Lahabi, and J. Aarts. Colossal proximity effect in a superconducting triplet spin valve based on the half-metallic ferromagnet CrO₂. *Phys. Rev. X* **5**, 021019 (2015).
- [5] S. Mironov and A. Buzdin. Triplet proximity effect in superconducting heterostructures with a half-metallic layer. *Phys. Rev. B* **92**, 184506 (2015).
- [6] P. Berghuis and P. H. Kes. Two-dimensional collective pinning and vortex-lattice melting in *a*-Nb_{1-x}Ge_x films. *Phys. Rev. B* **47**, 262–272 (1993).
- [7] Y. Fominov, N. Chtchelkatchev, and A. Golubov. Nonmonotonic critical temperature in superconductor/ferromagnet bilayers. *Phys. Rev. B* **66**, 014507 (2002).
- [8] J. Aarts, J. Geers, E. Bruck, A. Golubov, and R. Coehoorn. Interface transparency of superconductor/ferromagnetic multilayers. *Phys. Rev. B* **56**, 2779 (1997).
- [9] Z. Radovic, L. Dobrosavljevicgrujic, A. Buzdin, and J. Clem. Upper critical fields of superconductor-ferromagnet multilayers. *Phys. Rev. B* **38**, 2388 (1988).
- [10] B. Krunavakarn and S. Yoksan. Upper critical fields of ferromagnet/superconductor layered structures. *Physica C* **440**, 25 (2006).
- [11] A. Bezryadin. *Appendix A: superconductivity in MoGe alloys* (pp. 215–215). Wiley-VCH Verlag GmbH & Co. KGaA (2012).
- [12] A. Sidorenko, C. Surgers, and H. von Lohneysen. Perpendicular upper critical field of a proximity-coupled superconducting film. *Physica C* **370**, 197 (2002).

